FALSE ALARM PROBABILITIES FOR MIXED EVENTS

T. J. Cohen, et al

Teledyne Geotech

Prepared for:

Defense Advanced Research Projects Agency

5 November 1973

Unclassified

SECURITY CLASSIFICATION OF THIS PAGE *(When Data Entered)*

REPORT DOCUMENTATION PAGE	READ INSTRUCTIONS BEFORE COMPLETING FORM
1. REPORT NUMBER: SDAC-TR-73-8	2. GOVT ACCESSION NO.
3. RECIPIENT'S CATALOG NUMBER: AD 775 635	
4. TITLE *(and Subtitle)*: FALSE ALARM PROBABILITIES FOR MIXED EVENTS	5. TYPE OF REPORT & PERIOD COVERED: Technical
	6. PERFORMING ORG. REPORT NUMBER
7. AUTHOR(s): Cohen, T. J., Sweetser, E. I.	8. CONTRACT OR GRANT NUMBER(s): F08606-74-C-0006
9. PERFORMING ORGANIZATION NAME AND ADDRESS: Teledyne Geotech, 314 Montgomery Street, Alexandria, Virginia 22314	10. PROGRAM ELEMENT, PROJECT, TASK AREA & WORK UNIT NUMBERS
11. CONTROLLING OFFICE NAME AND ADDRESS: Defense Advanced Research Projects Agency, Nuclear Monitoring Research Office, 1400 Wilson Blvd. Arlington, Va. 22209	12. REPORT DATE: 5 November 1973
	13. NUMBER OF PAGES: 60
14. MONITORING AGENCY NAME & ADDRESS *(if different from Controlling Office)*: VELA Seismological Center, 312 Montgomery Street, Alexandria, Virginia 22314	15. SECURITY CLASS. *(of this report)*
	15a. DECLASSIFICATION DOWNGRADING SCHEDULE

16. DISTRIBUTION STATEMENT *(of this Report)*

APPROVED FOR PUBLIC RELEASE; DISTRIBUTION UNLIMITED.

17. DISTRIBUTION STATEMENT *(of the abstract entered in Block 20, if different from Report)*

18. SUPPLEMENTARY NOTES

19. KEY WORDS *(Continue on reverse side if necessary and identify by block number)*

Mixed-Event Analysis
Explosion Masking
False Alarm Probabilities

20. ABSTRACT *(Continue on reverse side if necessary and identify by block number)*

Analysis of 1,471 P- and PKP-coda indicates that the probability of an unexplained phase occurring in a coda of an event as recorded at a single station is 0.12 for a detection threshold on the order of 3.5db (signal-to-coda background). The average coda length is roughly 6 minutes (343 seconds) for the events examined. The probability, therefore, that the seismograms at four stations out of thirteen will exhibit unexplained phases in the coda of a

DD FORM 1 JAN 73 1473 EDITION OF 1 NOV 65 IS OBSOLETE

Unclassified

SECURITY CLASSIFICATION OF THIS PAGE *(When Data Entered)*

given earthquake is 0.045. That unexplained phases at four stations will yield a significant location solution (absolute values of the residual travel-time errors $|\varepsilon_i|$ less than 3 seconds) will occur with probability 0.032. Thus, with about 10,000 events occurring each year of magnitude $m_b \geq 4.0$, and with all of them examined for unexplained phases, we expect 15 false alarms per year. The probability that four or more stations will experience a false alarm is essentially the same as the probability that exactly four stations will experience a false alarm. For purposes of on-site inspection, residual travel-time errors $-3 \leq \varepsilon_i \leq 3$ seconds imply that an event can be located anywhere in an area 3.2×10^5 km^2 in size.

FALSE ALARM PROBABILITIES FOR MIXED EVENTS

Seismic Data Analysis Center Report No.: SDAC-TR-73-8

AFTAC Project No.:	VELA VT/4709
Project Title:	Seismic Data Analysis Center
ARPA Order No.:	1620
ARPA Program Code No.:	3F10
Name of Contractor:	TELEDYNE GEOTECH
Contract No.:	F08606-74-C-0006
Date of Contract:	01 July 1973
Amount of Contract:	$2,152,172
Contract Expiration Date:	30 June 1974
Project Manager:	Robert G. Van Nostrand (703) 836-3882

APPROVED FOR PUBLIC RELEASE: DISTRIBUTION UNLIMITED.

P. O. Box 334, Alexandria, Virginia 22314

TABLE OF CONTENTS

LIST OF FIGURES

LIST OF TABLES

LIST OF TABLES (Continued)

INTRODUCTION

With roughly ten thousand events of $m_b \geq 4.0$ occurring each year, the possibility exists that short-period signals from an explosion or an earthquake will be masked in the coda of another earthquake. When the signals are masked at only a few stations, detection is often possible. If, however, the short-period signals from an event are masked at all stations, it seems likely (due to the high background level on long-period records, and to the persistence of motion from large events) that the long-period signals will also be masked. If this occurs, detection is not possible. Obviously, then, some attempt should be made to search the secondary portions of seismograms for phases which may indicate the presence of a new event.

While simple in principle, the search of the coda of an event for secondary arrivals is fraught with difficulties. Though Cohen, et al. (1972) have demonstrated that coda characteristics are controlled primarily by the arrival times of predictable secondary phases (e.g., PP, PcP, etc.), numerous signal-like excursions within a given coda cannot be explained in terms of least-time paths through the earth. These unexplained phases may be thought of as "alarms" in the sense that their existence will cause a more thorough search of the pertinent seismograms to be made for other indications of a masked event. Most often the phase will go unexplained. In a larger

context, however, we would almost certainly want evidence of a second event on the seismograms at four or more stations, so that the event epicenter can be determined. The ability to locate the second event is important if coda suppression techniques such as the beam and mixed-signal processor (Dean et al., 1968) are to be used for enhancement of the masked signal. Thus, we are concerned with location solutions obtained using random, unexplained phases. Specifically, we are concerned with the number of significant location determinations obtained for nonexistent events; that is, the false alarm probabilities for mixed events.

In determining false alarm probabilities, we proceeded as follows. About 1500 P and PKP-codas were searched for phases which exceed a given amplitude threshold. These phases were first purged of known secondary arrivals (e.g. PP, PcP, etc.). The ratio of the number of unexplained arrivals to the number of coda examined, then, determined the probability of an unexplained phase occurring at a single station. The binomial theorem was subsequently used to determine the probability P_4 of having unexplained arrivals in a given event's coda at four stations out of a world-wide network of N stations. That these unexplained arrivals yield a significant location solution will occur with probability P_{L4}. The product of P_4 and P_{L4} then yields the probability that four stations of the world-wide network will experience a false alarm.

METHOD

Assume that the probability of an unexplained phase occurring in a coda of length T is P_o. Then, for a network of N stations, the probability P_s that four or more stations will have unexplained phases for a given event is:

$$P_s = \frac{N(N-1)(N-2)(N-3)}{4\cdot3\cdot2\cdot1} P_o^{\,4}(1-P_o)^{N-4} + \frac{N(N-1)(N-2)(N-3)(N-4)}{5\cdot4\cdot3\cdot2\cdot1} P_o^{\,5}(1-P_o)^{N-5} + \ldots = P_4 + P_5 + \ldots \quad (1)$$

If $P_{LN}(N\geq4)$ is the probability that unexplained phases observed for a given event at N stations will yield a significant location solution, the probability P_{FA} of a false alarm is

$$P_{FA} = P_4 \cdot P_{L4} + P_5 \cdot P_{L5} + \ldots \quad (2)$$

DATA

The first quantity to determine is the probability P_o of an unexplained phase occurring at a single station. To do this, we use the P and PKP coda determinations compiled by Cohen, et al. (1972). Specifically, for "arrivals" which exceed a given threshold amplitude, we will examine the number of unexplained phases present in the coda.

The method used to determine the coda decay characteristics is shown in Figure 1. Amplitude measurements, scaled relative to the largest excursion in the P or PKP coda, were made in a specified set of successive time windows. Measurements were made until the coda decayed into the pre-existing ambient noise level, or until a period of fifteen minutes had elapsed from the time of coda onset. In a few cases, measurements terminated with the arrival of a second event. The principal coda maxima were next plotted on log-linear paper, and the coda envelope obtained by connecting successive determinations. For example, the coda measurements of Figure 1 yield the coda envelope shown in Figure 2. Using the records from seventeen World Wide Standard Seismograph Stations whose locations are shown in Figure 3, Cohen, et al. (1972) determined the coda characteristics for events from the fifteen seismic regions shown in Figure 4; examples of typical coda decay characteristics are shown in Figure 5.

The following example illustrates the method used to flag suspect phases in the coda. As shown in Figure 2, we assume the log-coda decays linearly, and draw a line to connect the observations plotted at 40 and 60 seconds elapsed time. The relative ground motion at 50 seconds is then predicted, yielding a value of about 30%. The observed value, however, is 50%; as such, the signal-to-coda ratio r (observed-to-predicted) is 1.67 (4.5 db). Had we set a detection threshold ratio r of 1.5 (3.5 db), the arrival plotted at 50 seconds would be flagged for subsequent analysis. If this arrival is not found to be a predictable secondary phase (i.e., pP, PP, PcP, SKP, etc.), it is considered a false alarm. Obviously, recourse to the travel-time tables for body wave and surface wave phases, and to the actual seismograms, is required to purge the flagged arrivals of predictable phases. Note that no relationship exists between the detection threshold r and relative event size. To see this we need only consider that the earthquake and the event masked may be at different distances from the receiver, or that the event masked may appear anywhere in the coda of the earthquake.

Examples of false alarm analyses are shown in Tables I and II. By computing all observed-to-predicted coda ratios, cumulative figures for unexplained phases may easily be obtained for any given threshold ratio. In this work we analyze only those phases for which the detection ratio is $\geq$ 1.5. Using 1,471 P and PKP coda determinations, coda search and

analysis techniques yield the unexplained phases listed in Tables III through XVII. In general, these phases can be ascribed to the following phenomena:

A. Pulsing (Figure 6a)

Pulsing is taken to mean any large (in comparison to the background level) phase or excursion in the coda which is not a predictable arrival.

B. Normal Coda decay characteristics (Figure 6b)

Coda amplitudes rise and fall in the natural course of decay. These undulations are often large enough to produce an unexplained phase as we have defined this term. An example of this phenomena is the set of coda determinations (70%, 70%, 30%), which yields a detection ratio of 1.60 (4.1 db). Natural decay characteristics in a coda are generally identified as such by an experienced analyst, and would probably be dismissed from further consideration.

To be uniform in our treatment of the data, we include all unexplained phases - regardless of their character - in our compilation.

A summary of the phase analyses is shown in Table XVIII. For a detection threshold ratio of 1.5 (3.5 db), the data yield 175 unexplained phases in 1,471 events. Thus, the probability P_o of such a phase occurring at a single station is 0.118 or roughly one unexplained phase for every ten events. If we consider only those detections for which the threshold is 2.0 (6.0 db),

the single-station probability drops to .00816, or less than one unexplained phase for every 100 events. In both cases the average coda length $\bar{T}$ is 343 seconds (~6 minutes).

Table XX summarizes the results for the random location analyses. For any given trial, a random set of four stations is chosen from the available world-wide network (complete network shown in Table XIX). For each set of four stations, random times between 0 and T (T = 6 or 10 minutes) are added to the arrival times associated with an event at the center of the region specified. The altered arrival times are then used to determine a new surface-focus epicenter. If the absolute value of each station's residual travel-time error $|\varepsilon_i|$ is less than a specified value (here, 3 or 6 seconds), the location is considered acceptable, or "significant". As an example, the analysis performed for the Tadzhik-Hindu Kush region using 10 minute coda yields 50 acceptable solutions in 4505 trials ($|\varepsilon_i| \leq$ 6 seconds); thus, $P_{L4} = 0.011$. The significant location solutions are shown in Figure 7; by chance, one of the location solutions is for a non-existent event in Novaya Zemlya. The randomly derived location most remote from the reference epicenter (34°N, 73°E) is located 5582 km to the northwest, at coordinates (55°N, 6°E).

RESULTS

Results of the false alarm analyses are summarized in Table XXI. In computing false-alarm probabilities, we assume that a thirteen-station network is used for monitoring purposes (see Appendix).

For a detection threshold of r = 1.5 (3.5 db), a 6 minute coda, and a value $|\epsilon_i| \leq 6$ seconds, a thirteen-station world-wide network would experience 1.5 false alarms per 1,000 events. With roughly 10,000 events of magnitude $m_b \geq 4.0$ occurring each year, the network would experience 15 false alarms per year. However, many of the events with magnitudes on the order of 4.0 will have coda lengths much less than 6 minutes, resulting in fewer false alarms. If $|\epsilon_i| \leq 3$ seconds. the false alarm rate drops by a factor of 2, to about 7 false alarms per year.

False alarm rates for 10 minute coda (r = 1.5) are similar to the above. While the probability P_{L4} of four, random unexplained phases yielding a significant location solution decreases with increasing coda length, the assumption of a uniform distribution in the occurrence of unexplained phases results in an increase in P_4. Thus, the data of Table XXI suggest that for r = 1.5 and an increase in coda lengths to 10 minutes, the product of the probabilities P_4 and P_{L4} increases slightly, but by a factor less than 2.0. For 10 minute coda and $|\epsilon_i| \leq 6$ seconds, then, we expect about 17 false alarms per year. For $|\epsilon_i| \leq 3$

seconds, the false alarm rate drops to 9 false alarms per year.

At a detection threshold of 2.0 (6 db), false alarms are virtually eliminated.

While the probabilities P_{L4} determined for the Tadzhik-Hindu Kush region were used for the computations of false alarm probabilities (Table XXI), use of the P_{L4} determined for the Philippine Islands or the Kamchatka Peninsula would not significantly alter the results.

The false alarm probability for four or more stations is essentially the same as that for exactly four stations. To see this, consider a case for coda lengths of 6 minutes and r = 1.5; from Table XXI, we note that $P_o = 0.118$. Thus, for a thirteen station worldwide network, we find from equation (1) that $P_5 = 0.24\ P_4$. Now, requiring that five stations with random arrival times yield a significant location solution is a more severe restriction than requiring four stations to produce such a location. Thus, as seen in Tables XXa and b for the Kamchatka Peninsula data, $P_{L5} = .04\ P_4$ ($|\epsilon_i| \leq 6$ seconds). Taken together, the probability that a four or five station network will experience a false alarm is approximately 1% greater than the probability of a four station network experiencing a false alarm. Contributions for sub-networks of six or more stations will be even less. Thus, our estimates for the probability of a false alarm at four

stations are for all practical purposes the same as the false-alarm probability for four or more stations.

DISCUSSION

Basic to the problem of determining false alarm probabilities for mixed events is the question of what detection threshold is to be used for phase detection. We have seen that for a coda length of 6 minutes, a threshold of r = 1.5 (3.5 db) yields about 15 false alarms per year for $|\epsilon_i| \leq 6$ seconds and 7 false alarms per year for $|\epsilon_i| \leq 3$ seconds. At r = 2.0 (6.0 db), false alarms are virtually eliminated. It appears, then, that a network can be operated with r = 1.5, or perhaps slightly lower, without unreasonable false alarm occurrence.

It should also be noted that the number of unexplained phases occurring in the P coda at the various stations of a world-wide network is quite sensitive to the choice of a threshold level. As we have seen from Table XVIII, decreasing the threshold from r = 2.0 to r = 1.5 increases the number of unexplained phases by more than an order of magnitude (12 versus 175 unexplained phases for 1,471 coda observations). These observations suggest that the threshold used for phase detection in the coda of an event be in the neighborhood of r = 1.5, but probably no lower.

Given that time picks made in the secondary portions of seismograms are subject to considerable error, even a consistent set of arrival times for a masked event may yield an estimated location error of several hundred kilometers. For reasons related to on-site

inspection, therefore, let us inquire into the location uncertainty implied by residual travel-time errors ε_i for which $|\varepsilon_i| \leq 6$ and 3 seconds.

In determining the area associated with specified arrival-time errors, we randomly perturb the known travel times for a given event to four stations selected at random from a world-wide network, and examine the scatter in the location solutions. Details of this analysis are given in the Appendix. From the Appendix, we find the travel-time errors δ_i for which $-6 \leq \delta_i \leq 6$ imply that an event can be located anywhere in an area 3.2×10^5 km^2 in size (95% confidence level). Further, the location analysis shown in the Appendix suggests that errors in the travel-time picks less than or equal to $|\delta_i|$ imply residual travel-time errors ε_i such that $|\varepsilon_i| \simeq |\delta_i|/2$. Thus, the 3.2×10^5km^2 area of uncertainity should be associated with residual travel-time errors $-3 \leq \varepsilon_i \leq 3$ seconds. If $|\varepsilon_i| \leq 6$ seconds, $|\delta_i| \leq 12$ seconds, and the area of uncertainity is about 4 times larger, or 1.3×10^6 km^2. Similarly, if $|\varepsilon_i| \leq 1.5$ seconds, $|\delta_i| \leq 3$ seconds, and the area of uncertainity is roughly 8.0×10^4 km^2.

CONCLUSIONS

1. Using 1,471 P and PKP coda determinations (Cohen, et al., 1972) coda analysis yields the following:

Detection threshold (r)	Phases flagged	Unexplained Phases
1.5 (3.5 db)	990	175
2.0 (6.0 db)	446	12

In general, unexplained phases resulted from pulsing (unpredictable excursions in the coda) and normal coda undulations. The average coda length for the events studied was about 6 minutes (343 seconds).

2. The probability P_o of an unexplained phase occurring in a 6-minute coda at a single station is 0.12 for r = 1.5 (3.5 db). Thus, the probability P_4 that four stations out of thirteen will have unexplained phases in the coda of a given earthquake is 0.045. As the probability that unexplained phases at four stations will yield a significant location solution if 0.032 for residual travel-time errors $-3 \leq \varepsilon_i \leq 3$ seconds, the probability of a false alarm occurring is 0.0015 per event. This is equivalent to about 15 false alarms each year.

3. The false alarm probability for four or more stations is essentially the same as the false alarm probability for four stations.

4. For a detection threshold of 2.0 (6.0 db), false alarms are virtually eliminated.

5. The threshold used for phase detection should be in the neighborhood of r = 1.5 (3.5 db), but probably no lower.

6. For purposes of on-site inspection, residual travel-time errors $-3 \leq \varepsilon_i \leq 3$ seconds imply that an event can be located somewhere in an area 3.2×10^5 km^2 in size (95% confidence level).

7. If residual travel-time errors are such that $-1.5 \leq \varepsilon_i \leq 1.5$ seconds, the false alarm rate drops by a factor of 2, to 7 false alarms per year for r = 1.5. The corresponding area of uncertainity for location purposes is reduced by a factor of 4, to 8.0×10^4 km^2 (95% confidence level).

ACKNOWLEDGEMENTS

Discussions with Dr. R. Blandford on the subject of network false alarms are gratefully acknowledged. We also thank Messrs. T. Dutterer, A. Hill, and H. Husted for their assistance in performing the computations.

REFERENCES

Cohen, T. J., Sweetser, E. I., and Dutterer, T. J., 1972, P and PKP coda decay characteristics for earthquakes, Seismic Data Laboratory Report No. 301, Teledyne Geotech, Alexandria, Virginia.

Dean, W. C., Shumway, R. H., and Duris, C. S., 1968, Best linear unbiased estimation for multivariate stationary processes: Seismic Data Laboratory Report No. 207, Teledyne Geotech, Alexandria, Virginia.

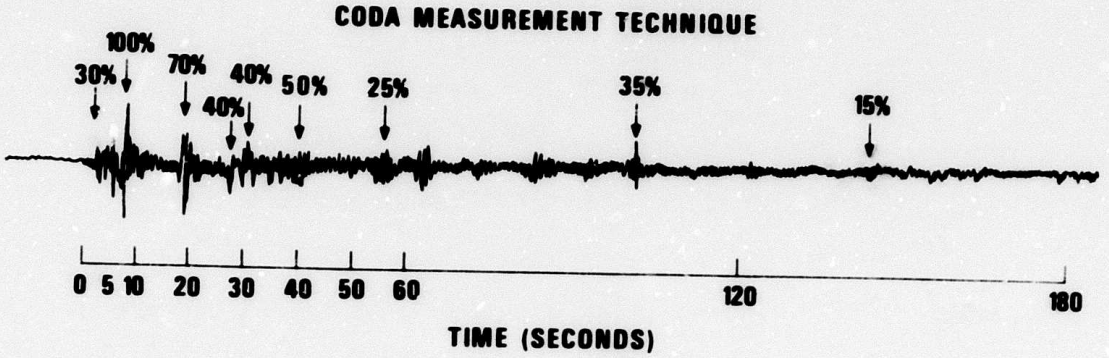

Figure 1. Coda measurement technique.

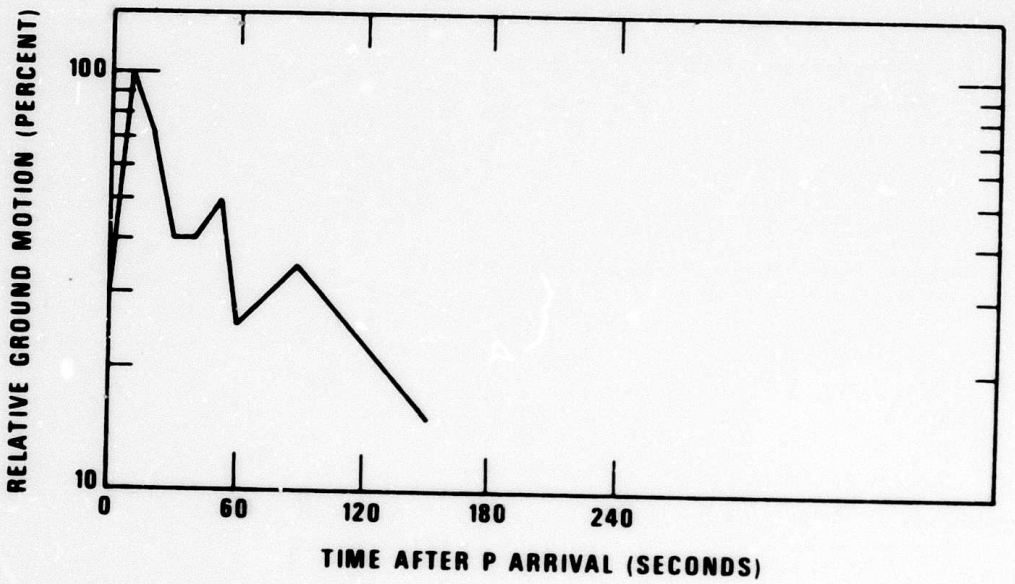

Figure 2. Single Coda determinations.

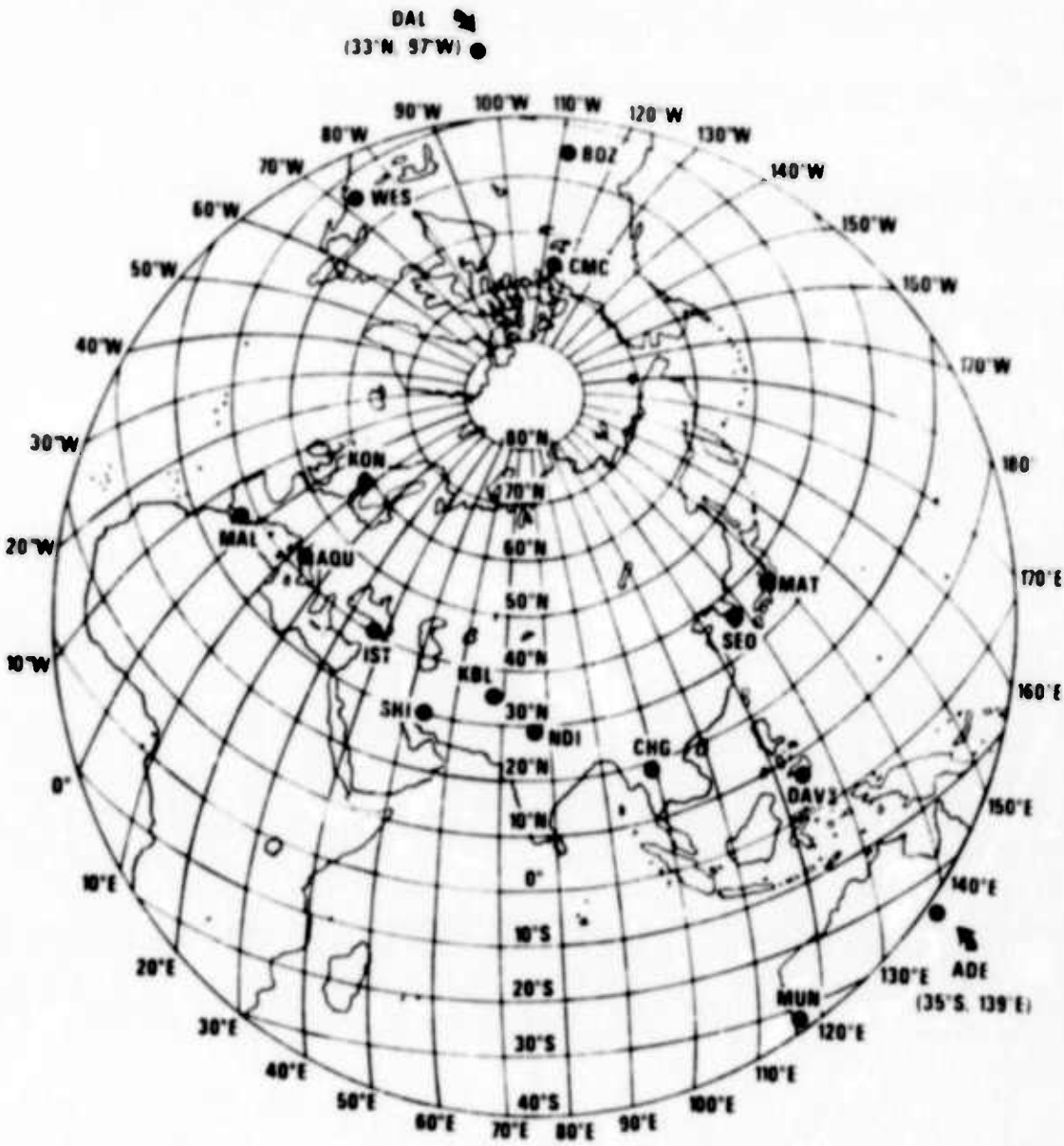

Figure 3. Map showing location of worldwide network.

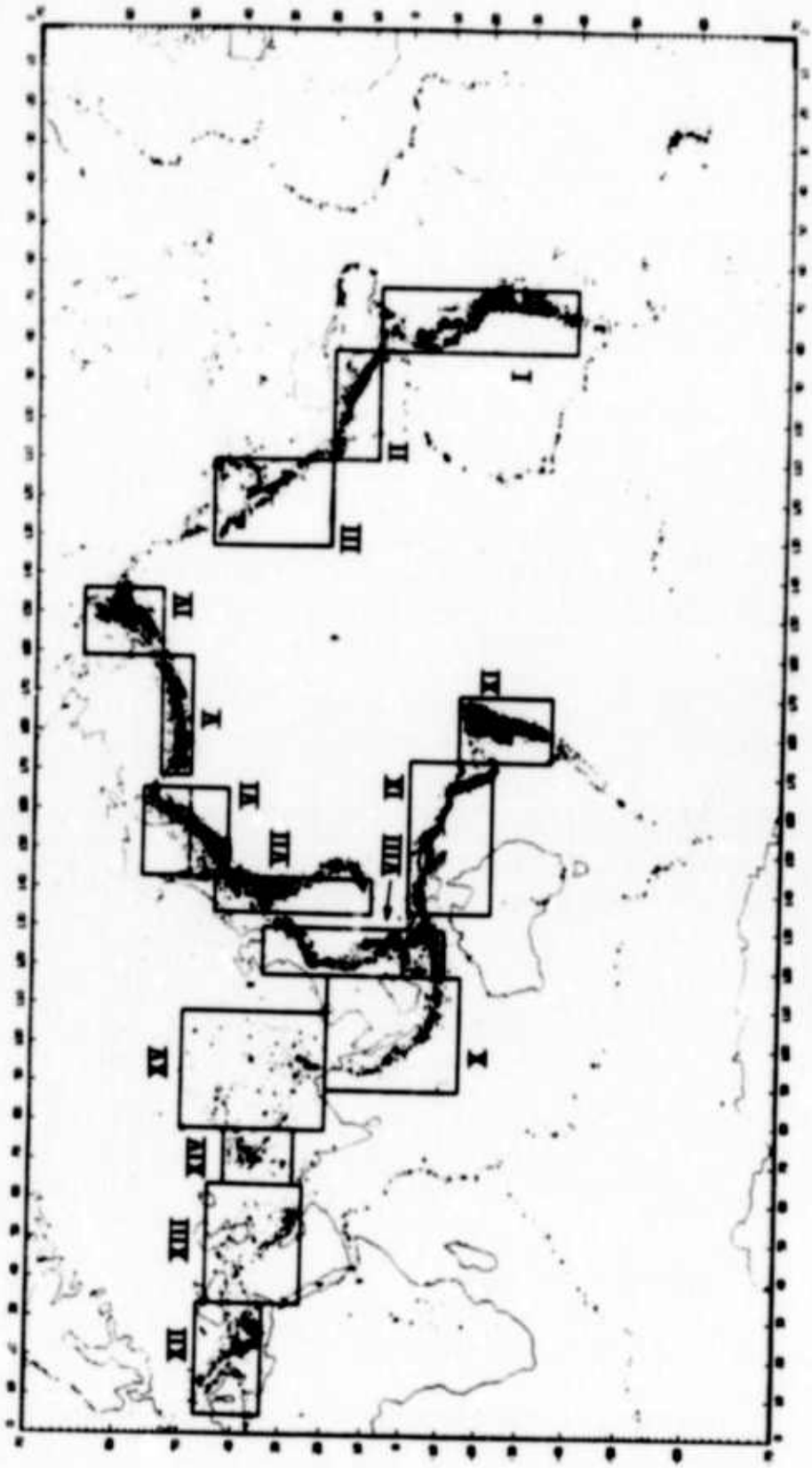

Figure 4. Regions used in coda analysis study.

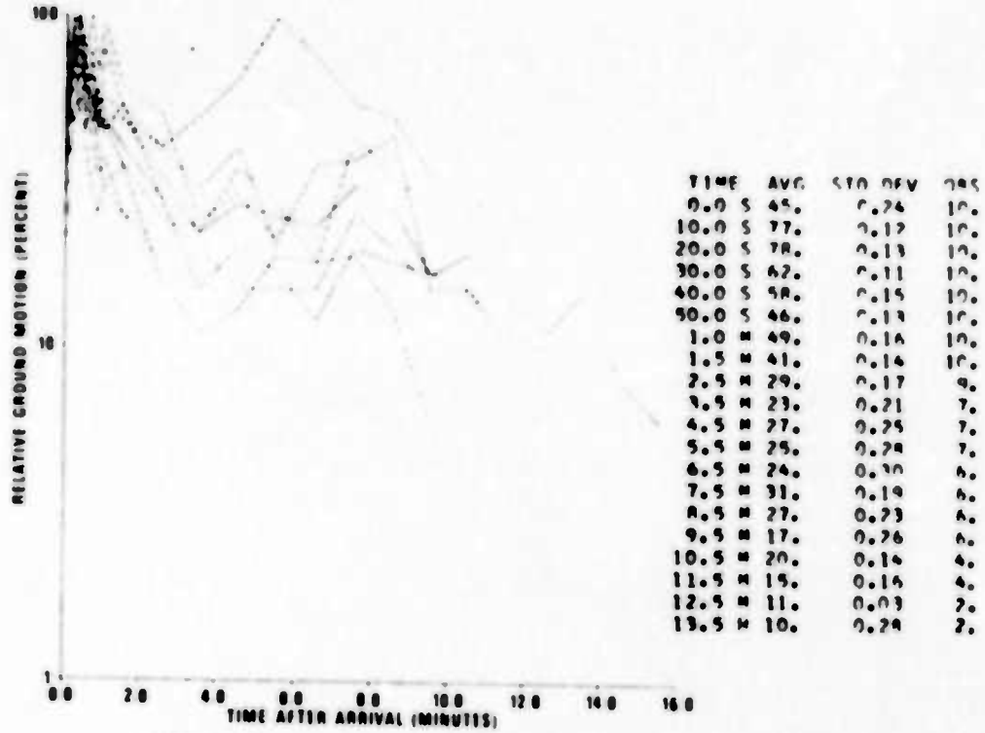

Figure 5a. P-coda, Alaska, CMC.

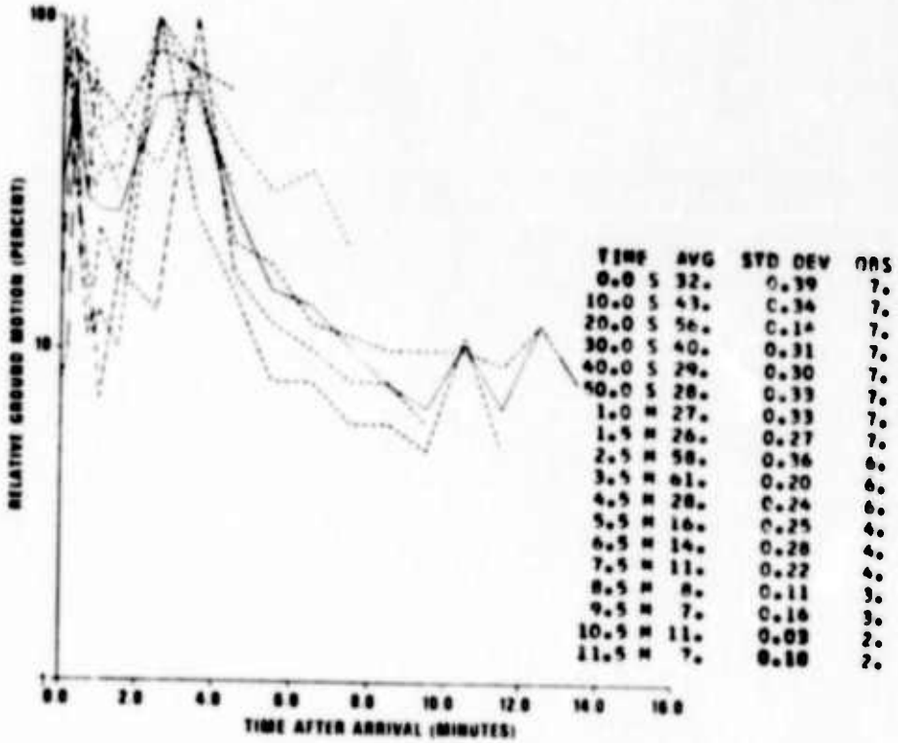

Figure 5b. PKP coda, Philippine Islands - Taiwan, WES.

Figure 5. Coda characteristics.

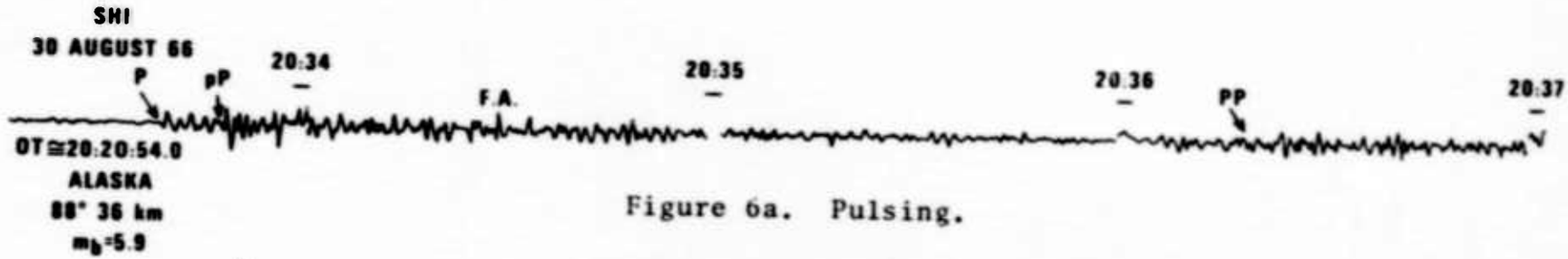

Figure 6a. Pulsing.

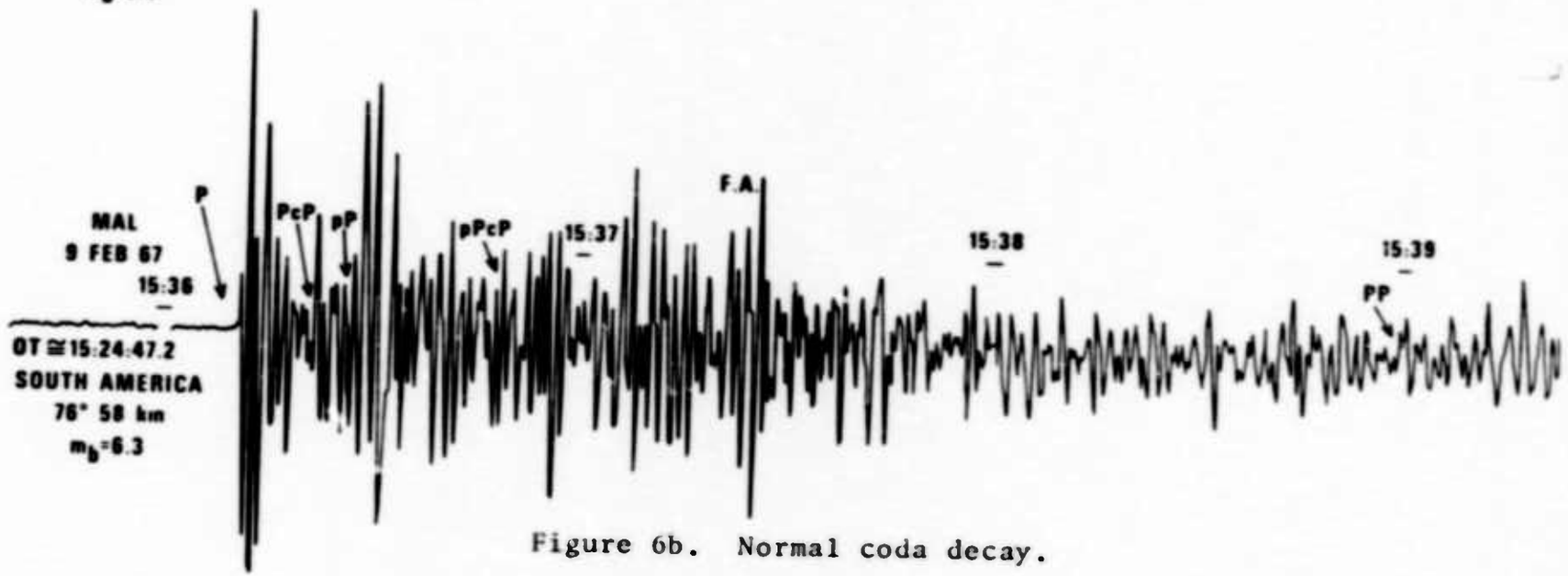

Figure 6b. Normal coda decay.

Figure 6. Unexplained phases.

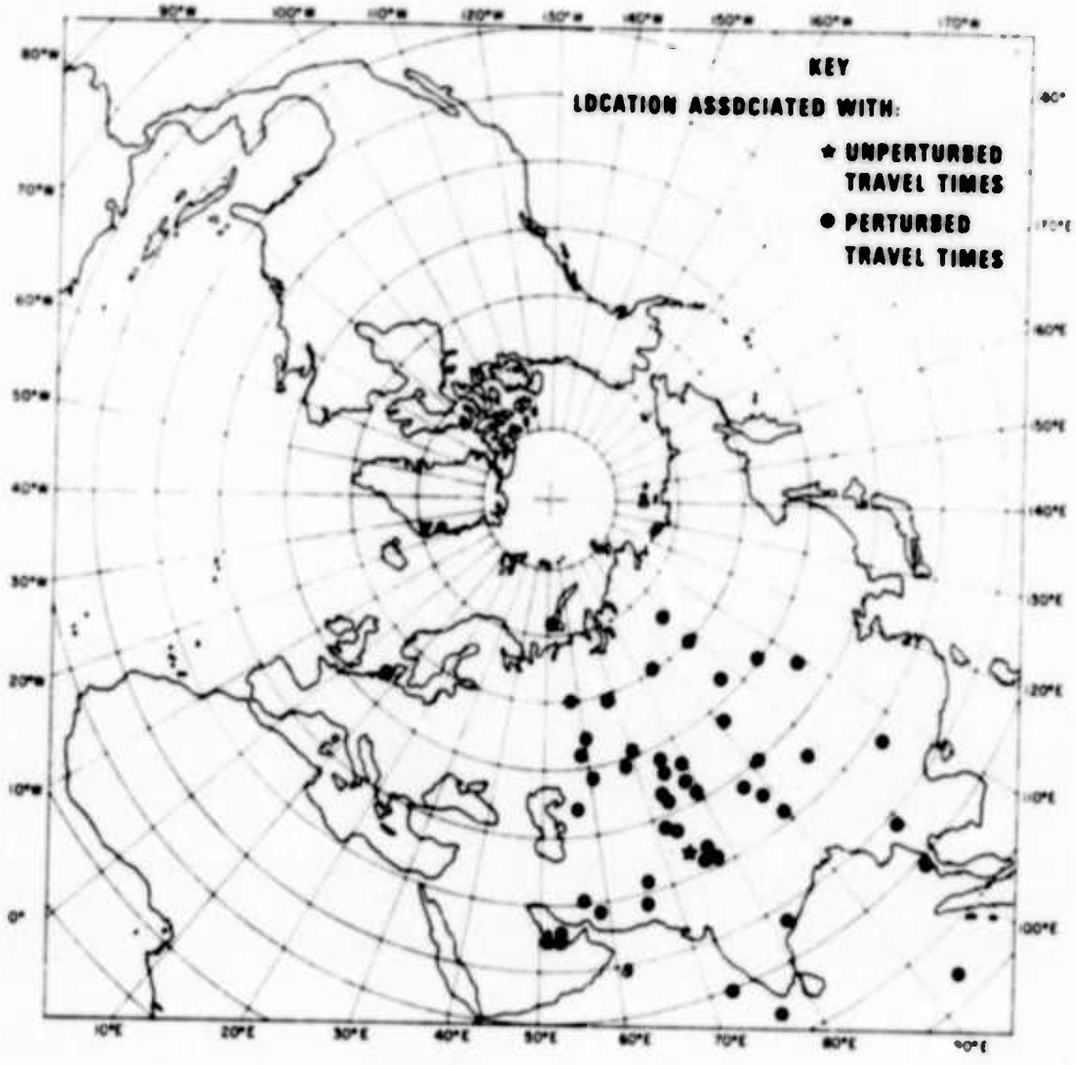

Figure 7. Significant location solutions, Tadzhik - Hindu Kush (10-minute coda, $-6 < \varepsilon_i < 6$ seconds).

TABLE I

Phase Analysis, P-Coda, CMC, Alaska,
11 April 1966 (18:26:11.8Z), $\Delta = 20°$

TIME INTERVAL s: seconds m: minutes	RATIO (Observed-To-Predicted)	COMMENTS
5-10s	0.79	
10-20s	1.34	
20-30s	0.92	
30-40s	1.25	
40-50s	0.58	
50-60s	1.71	Unexplained phase
1-2m	0.82	
2-3m	1.01	
3-4m	0.75	
4-5m	1.63	SS,SSS,PcP,Surface Waves

TABLE II

Phase Analysis, PKP-Coda, WES, Philippine Islands-Taiwan, 21 November 1965 (10:31:49.7Z), Δ = 139°

TIME INTERVAL s: seconds m: minutes	RATIO (Observed-to-Predicted)	COMMENTS
5-10s	0.98	
10-20s	0.80	
20-30s	1.15	
30-40s	0.57	
40-50s	1.88	pPKP
50-60s	0.71	
1-2m	1.19	
2-3m	0.59	
3-4m	1.83	SKP, PP
4-5m	0.92	
5-6m	0.78	
6-7m	1.43	

TABLE III

Unexplained Phases - South America

Station	Event Data (D-M-Y)	Origin Time (H-M-S)	Epicentral Distance (Deg.)	Time Interval in which False Alarm occurred s: seconds m: minutes	r Ratio of Observed-to-Predicted Coda Levels (r ≥ 1.5)	Comments
AQU	3 Sep 67	21:07:30.8	99°	50-60s	1.57	Pulsing, P
AQU	15 Nov 67	21:31:51.5	105°	30-40s	1.87	Pulsing,Weak Signal,P
CMC	27 Dec 67	09:17:55.7	95°	7-8 m	1.88	Pulsing, P
KON	21 Dec 67	02:25:21.6	103°	50-60s	1.68	Pulsing, P
MAL	18 Aug 64	04:44:58.0	89°	20-30s	1.52	Pulsing, P
MAL	9 Feb 67	15:24:47.2	76°	1-2 m	1.55	Pulsing, P
NDI	27 Jul 66	04:48:59.4	151°	1-2 m	2.36	Pulsing, PKP
NDI	15 Nov 67	21:31:51.5	152°	1-2 m	1.89	Pulsing, PKP
SHI	15 Feb 67	16:11;11.8	124°	30-40s	1.89	Pulsing, PKP
DAL	3 Sep 67	21:07:30.8	46°	30-40s	1.66	Pulsing, P
WES	4 Nov 67	16:26:48.2	45°	40-50s	1.77	Pulsing, P
WES	21 Dec 67	02:25:21.6	64°	5-6 m	1.57	Pulsing, P

TABLE IV

Unexplained phases - Central America

Station	Event Date (D-M-Y)	Origin Time (H-M-S)	Epicentral Distance = (Deg.)	Time Interval in which False Alarm Occurred s: seconds m: minutes	r Ratio of Observed-to-Predicted Coda Levels $r \geq 1.5$	Comments
ADE	6 Jul 64	07:22:11.7	125°	40-50s	1.63	Pulsing, PKP
ADE	25 Sep 66	06:02:26.4	125°	50-60s	1.86	Pulsing, PKP
AQU	3 Oct 67	18:16:03.2	90°	1-2 m	1.58	Pulsing, P
CHG	25 Sep 66	06:02:26.4	138°	40-50s	1.55	Pulsing, PKP
CMC	11 Apr 66	17:17:33.8	50°	30-40s	1.76	Pulsing, P
DAL	21 Mar 65	09:42:41.3	23°	1-2 m	1.79	Pulsing, P
DAV	23 Aug 65	19:46:02.9	133°	40-50s	1.54	Pulsing, PKP
MUN	25 Sep 66	06:02:26.4	144°	1-2 m	1.75	Pulsing, PKP
BOZ	15 Oct 67	08:00:50.3	40°	5-10s	1.66	Emerging, P

TABLE V

Unexplained phases - California and Western United States

Station	Event Date (D-M-Y)	Origin Time (H-M-S)	Epicentral Distance (Deg.)	Time Interval in which False Alarm occurred s: seconds m: minutes	r Ratio of Observed-to-Predicted Coda Levels ($r \geq 1.5$)	Comments
MAL	7 Aug 66	17:36:26.7	86°	30-40s	1.60	Pulsing, P
MAL	28 Dec 67	06:26:15.8	85°	30-40s	1.60	Pulsing,Weak Signal,P
MAT	9 Apr 68	02:28:58.9	82°	1-2 m	1.54	Pulsing, P
NDI	29 Apr 65	15:28:43.3	102°	50-60s	1.57	Normal Coda Decay, P

TABLE VI

Unexplained Phases - Alaska

Station	Event Date (D-M-Y)	Origin Time (H-M-S)	Epicentral Distance (Deg.)	Time Interval in which False Alarm occurred s: seconds m: minutes	r Ratio of Observed-to-Predicted Coda Levels ($r \geq 1.5$)	Comments
AQU	1 Jul 67	23:10:07.2	83°	40-50s	1.73	Pulsing, P
AQU	1 Jul 67	23:10:07.2	83°	9-10m	1.77	Normal Coda Decay, P
BOZ	7 Aug 66	14:11:51.2	24°	1-2 m	1.62	Pulsing, P
CHG	22 Dec 65	19:41:23.0	83°	40-50s	1.59	Normal Coda Decay, P
CHG	15 Aug 66	13:36:23.7	85°	40-50s	1.55	Pulsing, P
CMC	11 Apr 66	18:26:11.8	20°	50-60s	1.71	Pulsing, P
DAV	6 Feb 65	16:50:29.0	74°	1-2 m	1.50	Pulsing, P
DAV	22 Apr 66	23:27:20.5	80°	50-60s	2.39	Pulsing, P
DAV	23 Apr 68	20:29:14.5	81°	1-2 m	1.65	Pulsing, P
1ST	6 Feb 64	13:07:25.2	84°	6-7 m	1.71	Pulsing, P
KBL	15 Nov 68	00:07:09.7	82°	1-2 m	1.56	Pulsing, P
KBL	27 Nov 68	12:55:56.1	81°	1-2 m	1.55	Normal Coda Decay, P
KON	6 Feb 64	13:07:25.2	64°	1-2 m	1.60	Normal Coda Decay, P
KON	7 Oct 66	20:55:56.0	58°	30-40s	1.64	Pulsing, P
MAT	4 Sep 65	14:32:47.9	49°	30-40s	1.58	Pulsing, P
ND1	4 Sep 65	14:32:47.9	84°	1-2 m	1.90	Pulsing, P
NDI	22 Jan 66	14:27:07.9	85°	30-40s	1.66	Pulsing, P
ND1	23 Apr 68	20:29:14.5	85°	50-60s	1.81	Pulsing, P
SH1	22 Dec 65	19:41:23.0	90°	40-50s	1.71	Pulsing, P
SH1	30 Aug 66	20:20:54.0	88°	40-50s	1.51	Pulsing, P
SHI	7 Oct 66	20:55:56.0	87°	1-2 m	1.52	Pulsing, P

TABLE VII

Unexplained Phases - Aleutian Islands

Station	Event Dat. (D-M-Y)	Origin Time (H-M-S)	Epicentral Distance (Deg.)	Time Interval in which False Alarm Occurred s: seconds m: minutes	r Ratio of Observed-to-Predicted Coda Levels ($r \geq 1.5$)	Comments
ADE	4 Feb 65	05:01:21.8	93°	7-8 m	1.55	Normal Coda Decay, P
ADE	30 Mar 65	02:27:07.2	92°	1-2 m	1.63	Normal Coda Decay, P
ADE	23 May 65	23:46:12.0	92°	50-60s	1.50	Normal Coda Decay, P
AQU	7 Feb 65	02:27:09.2	85°	50-60s	1.72	Pulsing, P
AQU	17 Mar 65	14:27:12.4	83°	1-2 m	1.68	Normal Coda Decay, P
CHG	15 May 66	14:46:06.5	71°	1-2 m	1.99	Pulsing, P
CHG	11 Aug 66	10:45:59.6	76°	50-60s	1.71	Pulsing, P
DAL	1 Oct 65	08:52:05.8	63°	5-6 m	1.53	Normal Coda Decay, P
IST	1 Oct 65	08:52:05.8	85°	6-7 m	1.63	Normal Coda Decay, P
IST	29 Apr 67	03:55:20.8	85°	1-2 m	1.50	Normal Coda Decay, P
KBL	3 Oct 68	11:08:38.9	78°	1-2 m	1.59	Normal Coda Decay, P
KON	7 Feb 65	02:17:09.2	69°	50-60s	1.61	Pulsing, P
KON	23 May 65	23:46:12.0	68°	3-4 m	1.65	Normal Coda Decay, P
KON	1 Oct 65	08:52:05.8	70°	3-4 m	1.58	Normal Coda Decay, P
MAL	1 Oct 65	08:52:05.8	94°	40-50s	1.79	Pulsing, P
MAT	27 Sep 65	05:09:13.3	30°	20-30s	1.79	Pulsing, P
MUN	30 Mar 65	02:27:07.2	99°	30-40s	1.55	Pulsing, P
MUN	30 Mar 65	02:27:07.2	99°	7-8 m	1.51	Normal Coda Decay, P
ND1	1 Oct 65	08:52:05.8	75°	5-6 m	1.50	Normal Coda Decay, P
ND1	11 Aug 66	10:45:59.6	80°	50-60s	1.50	Normal Coda Decay, P
SEO	2 Jun 66	03:27:53.3	37°	30-40s	1.54	Pulsing, P
SEO	11 Aug 66	10:45:59.6	46°	40-50s	1.50	Normal Coda Decay, P
SH1	23 May 65	23:46:12.0	84°	1-2 m	1.72	Pulsing, P
SH1	1 Oct 65	08:52:05.8	87°	30-40s	1.51	Pulsing, P

TABLE VIII

Unexplained Phases - Kamchatka - Kurile Islands

Station	Event Date (D-M-Y)	Origin Time (H-M-S)	Epicentral Distance (Deg.)	Time Interval in which False Alarm occurred s:seconds m:minutes	r Ratio of Observed-to-Predicted Coda Levels ($r \geq 1.5$)	Comments
ADE	8 Apr 66	01:46:44.9	87°	40-50s	1.50	Normal Coda Decay, P
BOZ	18 Nov 65	21:58:12.4	54°	30-40s	1.69	Pulsing, P
CHG	19 Mar 66	08:11:40.0	46°	50-60s	1.57	Pulsing, P
DAV	4 Jun 66	23:48:17.8	45°	40-50s	1.67	Pulsing, P
IST	18 Nov 65	21:58:12.4	77°	40-50s	1.59	Normal Coda Decay, P
KON	8 Apr 66	01:46:44.9	67°	20-30s	1.94	Pulsing, P
MAL	31 May 64	00:40:36.4	96°	1-2 m	1.52	Normal Coda Decay, P
MUN	31 May 64	00:40:36.4	80°	1-2 m	1.72	Pulsing, P
MUN	31 May 64	00:40:36.4	80°	6-7 m	2.00	Pulsing, P
SEO	5 Feb 66	16:16:01.0	24°	1-2 m	1.56	Normal Coda Decay, P
SHI	11 May 66	14:17:34.1	76°	1-2 m	1.76	Normal Coda Decay, P
WES	31 May 64	00:40:36.4	88°	50-60s	1.50	Normal Coda Decay, P

TABLE IX

Unexplained Phases - Japan

Station	Event Date (D-M-Y)	Origin Time (H-M-S)	Epicentral Distance (Deg.)	Time Interval In which False Alarm occurred s: seconds m: minutes	r Ratio of Observed-to-Predicted Coda Levels ($r \geq 1.5$)	Comments
ADE	17 Jan 67	11:59:31.5	73°	1-2 m	1.64	Pulsing, P
AQU	29 Mar 65	10:47:37.6	85°	30-40s	1.90	Pulsing, P
BOZ	8 Jan 66	22:39:17.9	76°	40-50s	1.64	Normal Coda Decay, P
CMC	8 Jan 66	22:39:17.9	62°	50-60s	1.61	Normal Coda Decay, P
DAL	29 Mar 65	10:47:37.6	88°	40-50s	1.78	Pulsing, P
IST	29 Mar 65	10:47:37.6	79°	30-40s	1.55	Normal Coda Decay, P
KON	17 Jan 67	11:59:31.5	75°	1-2 m	1.55	Pulsing, P
MAT	7 Feb 67	08:28:57.9	22°	50-60s	2.05	Pulsing, P
MUN	26 Aug 67	00:36:42.1	50°	30-40s	1.61	Pulsing, P
MUN	12 Jul 68	00:44:36.5	75°	1-2 m	1.51	Normal Coda Decay, P
ND1	12 Nov 65	17:52:24.1	54°	20-30s	1.63	Pulsing, P
SEO	29 Mar 66	02:17:38.5	19°	1-2 m	1.59	Normal Coda Decay, P
SHI	26 Aug 67	00:36:42.1	82°	50-60s	1.65	Pulsing, P
WES	29 Mar 65	10:47:37.6	92°	1-2 m	1.50	Pulsing, P

TABLE X

Unexplained Phases - Philippine Islands - Taiwan

Station	Event Date (D-M-Y)	Origin Time (H-M-S)	Epicentral Distance (Deg.)	Time Interval in which False Alarm occurred s: seconds m: minutes	r Ratio of Observed-to-Predicted Coda Levels ($r \geq 1.5$)	Comments
ADE	11 Jan 66	03:10:53.0	39°	30-40s	1.60	Pulsing, P
AQU	18 Jan 64	12:04:40.0	66°	40-50s	1.56	Pulsing, P
CMC	14 Sep 65	08:27:15.9	92°	30-40s	1.58	Pulsing, P
CMC	16 Nov 65	17:05:37.9	77°	1-2 m	1.79	Normal Coda Decay, P
CMC	1 Jul 66	05:50:39.2	78°	1-2 m	1.83	Pulsing, P
DAV	1 Jul 66	05:50:39.2	18°	1-2 m	1.59	Pulsing in PP, P
IST	22 Jun 66	20:29:03.6	99°	10-20s	1.85	Pulsing, P
IST	8 Sep 66	21:15:52.8	96°	50-60s	1.50	Pulsing, P
KON	18 Jan 64	12:04:40.0	80°	50-60s	1.66	Pulsing, P
KON	8 Sep 66	21:15:52.8	102°	1-2 m	1.51	Pulsing, P
NDI	1 Nov 64	12:26:06.2	55°	40-50s	1.64	Normal Coda Decay, P
NDI	21 Aug 66	05:00:26.8	51°	40-50s	2.05	Normal Coda Decay, P
SHI	11 Oct 64	21:15:03.9	72°	50-60s	1.52	Pulsing, P
SHI	11 Jan 66	03:10:53.0	70°	1-2 m	1.58	Normal Coda Decay, P

TABLE XI

Unexplained Phases - Solomon Islands - New Hebrides

Station	Event Date (D-M-Y)	Origin Time (H-M-S)	Epicentral Distance (Deg.)	Time Interval in which False Alarm occurred s: seconds m: minutes	r Ratio of Observed-to-Predicted Coda Levels ($r \geq 1.5$)	Comments
AQU	17 Nov 64	08:15:39.3	127°	50-60s	1.57	Pulsing, PKP
BOZ	17 Nov 64	08:15:39.3	99°	1-2 m	1.55	Normal Coda Decay, P
BOZ	16 Feb 66	03:18:27.2	96°	40-50s	2.11	Pulsing;Weak Signal, P
BOZ	1 Dec 66	04:56:58.2	94°	1-2 m	1.55	Pulsing, P
CMC	17 Nov 64	08:15:39.3	97°	30-40s	1.56	Pulsing, P
CMC	4 Feb 66	10:39:12.2	100°	10-20s	1.72	Pulsing, P
CMC	22 Feb 66	05:02:37.2	96°	40-50s	1.62	Pulsing, P
CMC	22 Feb 66	05:02:37.2	96°	1-2 m	1.78	Pulsing, P
CMC	1 Dec 66	04:56:58.2	98°	1-2 m	1.56	Normal Coda Decay, P
CMC	14 Dec 66	21:07:52.1	99°	40-50s	1.63	Pulsing, P
DAV	16 Feb 66	03:18:27.2	49°	30-40s	1.83	Pulsing, P
IST	7 Oct 66	15:55:10.8	142°	30-40s	1.59	Normal Coda Decay, PKP
KBL	10 Mar 69	06:54:17.6	83°	13-14m	1.73	Normal Coda Decay, P
MAT	14 Aug 65	11:07:47.1	59°	20-30s	1.56	Normal Coda Decay, P
NDI	15 Jun 66	01:32:55.5	90°	40-50s	1.63	Pulsing, P
SHI	13 Jun 66	18:08:38.4	117°	10-20s	1.56	Pulsing, PKP

TABLE XII

Unexplained Phases - Sumatra - Java

Station	Event Date (D-M-Y)	Origin Time (H-M-S)	Epicentral Distance (Deg.)	Time Interval in which False Alarm occurred s: seconds m: minutes	r Ratio of Observed-to-Predicted Coda Levels ($r \geq 1.5$)	Comments
BOZ	26 Feb 65	08:55:42.2	131°	20-30s	1.60	Pulsing, PKP
BOZ	24 Mar 67	09:00:19.5	125°	20-30s	1.56	Pulsing, PKP
KON	12 Apr 67	04:51:40.2	84°	1-2 m	2.35	Pulsing, P
KON	12 Apr 67	04:51:40.2	84°	6-7 m	1.63	Normal Coda Decay, P
NDI	29 Apr 65	15:48:57.1	47°	40-50s	2.65	Normal Coda Decay, P
NDI	7 Jun 65	10:18:57.0	41°	20-30s	1.55	Normal Coda Decay, P
SHI	30 Mar 67	02:08:02.4	73°	50-60s	1.51	Pulsing, P

TABLE XIII

Unexplained Phases - Tonga Islands - Fiji Islands

Station	Event Date (D-M-Y)	Origin Time (H-M-S)	Epicentral Distance (Deg.)	Time Interval in which False Alarm occurred s: seconds m: minutes	r Ratio of Observed-to-Predicted Coda Levels ($r \geq 1.5$)	Comments
BOZ	28 Aug 66	07:29:34.7	103°	1-2 m	1.72	Pulsing, P
CMC	1 Jan 67	07:05:48.6	93°	1-2 m	1.54	Pulsing, P
CMC	4 Mar 67	06:16:21.9	97°	10-20s	1.55	Pulsing, P
MAL	1 Jun 66	11:47:53.1	164°	20-30s	1.87	Pulsing, PKP
MAL	1 Jan 67	07:05:48.6	157°	1-2 m	1.60	Normal Coda Decay, PKP
MAT	17 Feb 67	10:10:51.5	74°	50-60s	1.53	Pulsing, P
SEO	17 Feb 67	10:10:51.5	82°	30-40s	1.92	Pulsing, P

TABLE XIV

Unexplained Phases - Turkey - Greece

Station	Event Date (D-M-Y)	Origin Time (H-M-S)	Epicentral Distance (Deg.)	Time Interval in which False Alarm occurred s: seconds m: minutes	r Ratio of Observed-to-Predicted Coda Levels ($r \geq 1.5$)	Comments
BOZ	5 Feb 66	02:01:48.3	86°	1-2 m	1.80	Pulsing, P
BOZ	5 Feb 66	02:01:48.3	86°	4-5 m	1.60	Pulsing, P
CMC	5 Feb 66	02:01:48.3	69°	5-6 m	1.50	Pulsing, P
CMC	29 Oct 66	02:39:29.4	68°	3-4 m	1.51	Pulsing, P
CMC	9 Feb 67	14:08:18.7	67°	7-8 m	1.50	Normal Coda Decay, P
DAL	9 Apr 65	23:57:03.2	93°	40-50s	1.53	Pulsing, P
DAL	9 Apr 65	23:57:03.2	93°	1-2 m	1.61	Pulsing, P
DAL	5 Feb 66	02:01:48.3	89°	50-60s	2.30	Pulsing, P
DAL	29 Oct 66	02:39:29.4	88°	30-40s	1.51	Pulsing, P
DAL	22 Jul 67	16:56:53.3	92°	10-20s	1.67	Normal P Build-Up, P
DAL	22 Jul 67	16:56:53.3	92°	50-60s	1.67	Pulsing, P
KON	30 Nov 67	07:23:51.5	19°	1-2 m	1.70	Pulsing, P
MAL	22 Jul 67	16:56:53.3	28°	2-3 m	1.58	Normal Coda Decay, P
MAL	30 Nov 67	07:23:51.5	20°	1-2 m	1.53	Pulsing, P
MAT	1 May 67	07:09:00.5	84°	1-2 m	1.65	Pulsing, P
MAT	22 Jul 67	16:56:53.3	78°	30-40s	1.79	Pulsing, P
MAT	22 Jul 67	16:56:53.3	78°	1-2 m	1.80	Pulsing, P
WES	9 Apr 65	23:57:03.2	71°	1-2 m	1.60	Normal Coda Decay, P

TABLE XV

Unexplained Phases - Iran - Turkey

Station	Event Date (D-M-Y)	Origin Time (H-M-S)	Epicentral Distance (Deg.)	Time Interval in which False Alarm occurred s: seconds m: minutes	r Ratio of Observed-to-Predicted Coda Levels ($r \geq 1.5$)	Comments
ADE	31 Aug 68	10:47:37.4	101°	20-30s	2.02	Pulsing;Weak Signal, P
ADE	31 Aug 68	10:47:37.4	101°	1-2 m	1.65	Pulsing;Weak Signal, P
CMC	11 Jan 67	11:20:45.7	77°	40-50s	1.55	Pulsing, P
KON	18 Sep 66	20:43:53.3	44°	40-50s	1.83	Pulsing, P
NDI	21 Jun 65	00:21:14.5	19°	1-2 m	1.53	Pulsing in PP, P
SEO	12 Jul 66	18:53:08.5	65°	1-2 m	1.63	Pulsing, P

TABLE XVI

Unexplained Phases - Tadzhik - Hindu Kush

Station	Event Date (D-M-Y)	Origin Time (H-M-S)	Epicentral Distance (Deg.)	Time Interval in which False Alarm occurred s: seconds m: minutes	r Ratio of Observed-to-Predicted Coda Levels ($r \geq 1.5$)	Comments
CMC	24 Jan 66	07:23:07.6	82°	40-50s	1.93	Pulsing, P
DAV	20 Feb 67	15:18:39.9	53°	20-30s	1.58	Normal Coda Decay, P
IST	16 Aug 66	02:16:19.7	33°	10-20s	1.52	Pulsing, P
MAT	25 Jan 67	01:50:19.4	52°	10-20s	1.84	Pulsing, P
SEO	1 Aug 66	19:09:55.1	48°	30-40s	1.59	Pulsing, P
SEO	25 Jan 67	01:50:19.4	44°	10-20s	1.70	Pulsing, P
SEO	20 Feb 67	15:18:39.9	42°	50-60s	2.26	Pulsing, P
SHI	5 Jan 66	20:45:54.6	16°	30-40s	1.53	Pulsing, P
WES	25 Jan 67	01:50:19.4	94°	30-40s	1.60	Pulsing;Weak Signal, P

TABLE XVII

Unexplained Phases - China- Nepal - Burma

Station	Event Date (D-M-Y)	Origin Time (H-M-S)	Epicentral Distance (Deg.)	Time Interval in which False Alarm occurred s: seconds m: minutes	r Ratio of Observed-to-Predicted Coda Levels ($r \geq 1.5$)	Comments
ADE	27 Jun 66	10:41:08.6	84°	30-40s	1.60	Pulsing, P
ADE	28 Sep 66	14:00:22.9	72°	50-60s	1.68	Pulsing, P
AQU	30 Aug 67	04:22:01.5	67°	5-6 m	1.60	Pulsing, P
BOZ	6 Mar 66	02:15:56.7	102°	50-60s	1.57	Pulsing, P
CMC	16 Dec 66	20:52:13.5	82°	1-2 m	1.70	Pulsing, P
DAV	5 Feb 66	15:12:29.1	29°	20-30s	1.83	Pulsing, P
IST	27 Jun 66	10:41:08.6	43°	50-60s	1.85	Pulsing, P
MAL	12 Jan 65	13:32:24.0	76°	50-60s	1.81	Pulsing, P
MAL	5 Feb 66	15:12:29.1	88°	30-40s	2.18	Pulsing;Weak Signal, P
MAL	5 Feb 66	15:12:29.1	88°	50-60s	1.86	Pulsing;Weak Signal, P
MAT	15 Aug 67	09:21:02.5	37°	30-40s	1.54	Pulsing, P
MUN	12 Jan 65	13:32:24.0	65°	1-2 m	1.60	Pulsing, P
NDI	5 Feb 66	15:12:29.1	23°	12-13m	1.63	Normal Coda Decay, P
SEO	14 Mar 67	06:38:04.6	29°	30-40s	1.54	Pulsing, P

TABLE XVIII

Summary of Phase Analysis

Area	Number of Coda Observations	Average Coda Length(sec)	Number of Phases Flagged r=2.0*	Number of Phases Flagged r=1.5*	Number of Unexplained Phases r=2.0*	Number of Unexplained Phases r=1.5*	Detection Ratio for Largest Arrival	Identified Phase	Largest Unexplained Phase Detection Ratio
South America	120	501	76	90	1	11	6.03	PKP-AB	2.36
Central America	89	451	48	60	0	9	10.91	SKP	1.86
California and Western U. S.	52	317	16	33	0	4	3.79	PP	1.60
Alaska	106	363	20	91	1	20	3.35	pP	2.39
Aleutians	99	291	26	75	0	24	4.24	ScP	1.995
Kamchatka and Kurile Is.	106	304	28	60	1	11	3.18	pP	2.00
Japan	115	357	41	75	1	13	4.47	PcP	2.05
Philippine Is. and Taiwan	108	342	36	91	1	13	6.73	SKP	2.03
Solomons and New Hebrides	123	387	25	115	1	15	5.45	ScP	2.11
Sumatra and Java	100	280	31	62	2	5	8.41	PcP, pP, PP	2.65
Tonga and Fiji Is.	117	220	31	41	0	7	5.77	PP	1.92
Turkey - Greece	85	372	22	64	1	17	4.81	PP	2.30
Iran - Turkey	72	352	11	35	1	5	3.94	pP	2.02
Tadzhik - Hindu Kush	92	273	15	38	1	8	3.90	S, Le	2.25
China - Nepal - Burma	87	332	20	60	1	13	3.16	PcP	2.18
Totals	1471	343	446	990	12	175			

* r is the detection threshold ratio:

r = 1.5 equivalent to a detection threshold of 3.5db.
r = 2.0 equivalent to a detection threshold of 6.0db.

TABLE XIX

World-Wide Network

Used for Random Location Analysis

Stations	Location	
	Latitude	Longitude
AA-AL	70.00N	160.00W
ADE	34.97S	138.71E
AGR	27.13N	78.02E
ALI	38.36N	0.49W
ANK	39.92N	32.82E
AQU	42.35N	13.40E
AT-TU	52.85N	173.17E
CHG	18.70N	98.98E
DAV	7.09N	125.57E
HK-JP	43.50N	145.50E
HN-ME	46.16N	67.99W
KBL	35.00N	75.00E
LAO	46.69N	106.22W
NOSR	61.05N	10.90E
NP-NT	76.25N	119.37W
SEO	37.57N	126.97E
SJ-TX	27.61N	93.31W
TE-IR	36.00N	52.00E
WY-AU	15.00N	127.00E

TABLE XXa

Random Location Analyses

Four Stations (N=4)

Region	Lat. (Deg)	Long. (Deg)	Coda Length (Min)	No. of Trials	Acceptable Solutions $\|c_i\| < 6$ seconds No. Solutions	P_{LN}	Acceptable Solutions $\|c_i\| < 3$ seconds No. Solutions	P_{LN}	Stations Used
Tadzhik - Hindu Kush	34N	73E	10	4595	50	1.11×10^{-2}	27	5.99×10^{-3}	AA-AL, ADE, AGR, ALI, ANK, AQU, AT-TU, CHG, DAV, HK-JP, HN-ME, KBL, LAO, NORSR, NP-NT, SEO, TE-IR
Tadzhik - Hindu Kush	34N	73E	6	2500	81	3.24×10^{-2}	40	1.60×10^{-2}	same as above
Phillipine Islands	12N	126E	6	1957	76	3.88×10^{-2}	39	1.99×10^{-2}	AA-AL, ADE, AGR, AT-TU, CHG, DAV, HK-JP, KBL, SEO, TE-IR
Kamchatka Peninsula	54N	156E	6	1637	51	3.12×10^{-2}	19	1.16×10^{-2}	AA-AL, ADE, AGR, ALI, ANK, AQU, AT-TU, CHG, DAV, HK-JP, HN-ME, KBL, LAO, NOSR, NP-NT, SEO, SJ-TX, TE-IR.

TABLE XXb

Five Stations (N=5)

Kamchatka Peninsula	54N	156E	6	1737	2	1.15×10^{-3}	0		AA-AL, ADE, AGR, ALI, ANK, AQU, AT-TU, CHG, DAV, HK-JP, HN-ME, KBL, LAO, NOSR, NP-NT SEO, SJ-TX, TE-IR

TABLE XXI

False Alarm Analysis

Threshold Ratio r*	Coda Length T(sec)**	Travel-Time Errors δ_i(sec)	Probability of Unexplained Phase at a Single Station P_o***	Probability of Unexplained Phases at Four Stations P_4	Probability of Four Unexplained Phases Yielding a significant Location Solution P_{L4}****	Probability of False Alarm for Four Stations $P_4 \cdot P_{L4}$
1.5	360	±6	1.18×10^{-1}	4.48×10^{-2}	5.24×10^{-2}	1.45×10^{-3}
1.5	360	±3	1.18×10^{-1}	4.48×10^{-2}	1.60×10^{-2}	7.18×10^{-4}
2.0	360	±6	8.16×10^{-3}	2.94×10^{-6}	5.24×10^{-2}	9.52×10^{-8}
2.0	360	±3	8.16×10^{-3}	2.94×10^{-6}	1.60×10^{-2}	4.71×10^{-8}
1.5	600	±6	1.97×10^{-1}	1.49×10^{-1}	1.11×10^{-2}	1.65×10^{-3}
1.5	600	±3	1.97×10^{-1}	1.49×10^{-1}	5.99×10^{-3}	8.32×10^{-4}
2.0	600	±6	1.56×10^{-2}	2.16×10^{-5}	1.11×10^{-2}	2.39×10^{-7}
2.0	600	±3	1.56×10^{-2}	2.16×10^{-5}	5.99×10^{-3}	1.29×10^{-7}

* r = 1.5 equivalent to a detection threshold of 3.5db
r = 2.0 equivalent to a detection threshold of 6.0db

** Nominal value; the average coda length $\bar{T}$ for the events analyzed is 345 seconds.

*** Determined for N = 13 (see Appendix)
Also, we assume a uniform distribution of unexplained arrivals such that the P_o determined for T=600 seconds are simply the P_o for T=360 seconds multiplied by a factor of (600/360).

**** Probabilities P_{L4} determined for the Tadzhik-Hindu Kush region, using four-station groups.

APPENDIX

Computation of the Average Location Area Associated With Specified Arrival Time Errors

We seek a determination of the area associated with specified errors in station arrival times.

For a given region outlined in Figure 4 (main text) the distances from the four corners of the region to each station listed in Table XIX (main text) were computed. If the distance between any one corner and a station exceeds 100°, this station is eliminated from the network. The P wave travel times from the center of the region to the remaining stations in the network are then computed. Using a random-number generator, four stations are selected from the network, and their travel times perturbed by random numbers of up to $\pm\delta_i$ seconds. Program SHIFT (Chiburis, 1968) is then used to obtain a surface-constrained location. In all, 20 location solutions using random sets of four stations and random travel-time perturbations are computed for each region.

Of these, one is deleted, yielding an estimate (at the 95% confidence level) of the location area A_k. Averaging over the A_k yields a world-wide estimate $\bar{A}$ for the location area. A typical plot of the locations obtained for random combinations of four stations and random sets of time perturbations is given in Figure A1 (Solomon Islands - New Hebrides). Here, we have assumed that arrivals can be picked to an accuracy of better than 6 seconds, that is, $-6 \leq \delta_i \leq 6$ seconds. We delete the solution at (6.5°S, 152.8°E), and enclose the remaining locations with a

rectangle centered at the true epicentral location (12°S, 156°E). This rectangle defines the area A_k in which 95% of all locations are assumed to fall. The area in Figure A1 is 7° high by 3° wide. Applying short-distance conversion factors (Richter, Appendix XII, 1958), the area is found to be 775 km high by 325 km wide; the area A_k, therefore, is 2.5×10^5 km^2.

A summary of the solutions for the A_k is given in Table AI. As noted, an insufficient number of stations was available for analysis of the South American region. Further, the determinations for the Philippine Is.-Taiwan region, and Turkey-Greece are questionable, as less than 19 solutions were available for analysis. Using the results for the 12 remaining regions yields an average area $\bar{A}$ of 3.2×10^5 km^2, with an average of 13 stations receiving P-wave arrivals from each region ($-6 \leq \delta_i \leq 6$ seconds). For $-3 \leq \epsilon_i \leq 3$ seconds, the area dimensions given in Table AI should be roughly halved. This may be seen from Table AII which shows the results of two sets of location analyses performed using random travel-time perturbations of up to ±3 and ±6 seconds. For a given region, the same 20 sub-networks of four stations were used, but the travel-time perturbations in each trial for which $-3 \leq \epsilon_i \leq 3$ seconds were exactly half of those used in the corresponding trial for which $-6 \leq \delta_i \leq 6$ seconds. In each case, the area dimensions for $-3 \leq \delta_i < 3$ seconds are about half of the dimensions obtained for

$-6 \leq \delta_i \leq 6$ seconds. Thus, for picking errors of up to ±3 seconds, the average location area $\bar{A}$ is on the order of 0.8×10^5 km^2.

As a final note, when determining the location of an event, the easiest way to estimate the accuracies of the travel-time picks would seem to be by examination of the residual travel-time errors ε_i for each station. To determine the experience relationship between residual travel-time errors ε_i and picking errors δ_i, let us compare these parameters for various location solutions computed using specified, random travel-time perturbations.

Figure A2 shows a comparison of residual travel-time errors ε_i and the specified (input) picking errors δ_i. We examine 19 location solutions for each of two regions; in both cases, $-6 \leq \delta_i \leq 6$ seconds. Of the 152 data pairs shown, 142, or 93% of the total, lie within the area bounded by $-3 \leq \varepsilon_i \leq 3$ seconds. A similar study for which $-3 \leq \delta_i \leq 3$ seconds (Figure A3) shows about 90% of the determinations to fall in the range $-1.5 \leq \varepsilon_i \leq 1.5$ seconds. Thus, the data suggest that travel-time errors less than or equal to $|\delta_i|$ imply residual travel-time errors ε_i such that $|\varepsilon_i| \simeq |\delta_i|/2$.

REFERENCES

Chiburis, E. F., 1968, Precision location of underground nuclear explosions using teleseismic networks and predetermined travel-time anomalies, Seismic Data Laboratory Report No. 214, Teledyne, Inc., 1 March.

Richter, C. F., 1958, Elementary Seismology, W. H. Freeman and Co., San Francisco.

TABLE AI

Area Analysis - Results

($-6 < \delta_i < 6$ seconds, unless noted)

Region	Number of Stations Receiving P Arrivals	X (km)	Y (km)	Area(A_k) $km^2 \times 10^5$	Comments
South America	3*				Insufficient Number of Stations
Central America	9	390	530	2.1	
California and Western, U.S.**	8	185	485	0.9	
Alaska	18	360	620	2.2	
Aleutian Islands	18	495	850	4.2	
Kamchatka-Kurile ls. $\binom{K}{KI}$	19	$\binom{695}{605}$	$\binom{590}{445}$	$\binom{4.1}{2.7}$	Area = 3.4×10^5 km^2
Japan	12	260	400	1.0	
Philippine Is-Taiwan**	11*	215	1455	3.1*	One solution, unstable due to network configuration
Solomon Is.-New Hebrides	7	325	775	2.5	
Sumatra - Java	11	600	1080	6.5	Some solutions unstable due to network Configuration
Tonga ls. - Fiji ls.	7	780	710	5.5	19 solutions; one deleted
Turkey - Greece	15*	1350	1445	19.5*	12 solutions, none deleted
Iran - Turkey	16	655	640	4.2	
Tadzhik - Hindu Kush	15	220	750	1.7	
China - Nepal - Burma	16	550	690	3.8	19 Solutions, none deleted
Average	13			3.2	$\bar{A} = 3.2 \times 10^5$ km^2

* Omit from computation of averages

** Obtained from data for which $-3 \leq \delta_i \leq +3$ seconds and adjusted to $-6 < \delta < 6$ seconds.

TABLE AII

Corresponding Location Analysis
for Picking Errors δ_i of up to ±3 and ±6 Seconds

Picking Errors	Area Dimensions* (95% Confidence Level) Latitude	Longitude	Region
Up to ±3 seconds	1.0°	1.4°	Kamchatka Peninsula
Up to ±6 seconds	1.4°	2.8°	Kamchatka Peninsula
Up to ±3 seconds	2.1°	2.9°	Kurile Islands
Up to ±6 seconds	4.7°	5.9°	Kurile Islands

* 20 solutions computed; one deleted

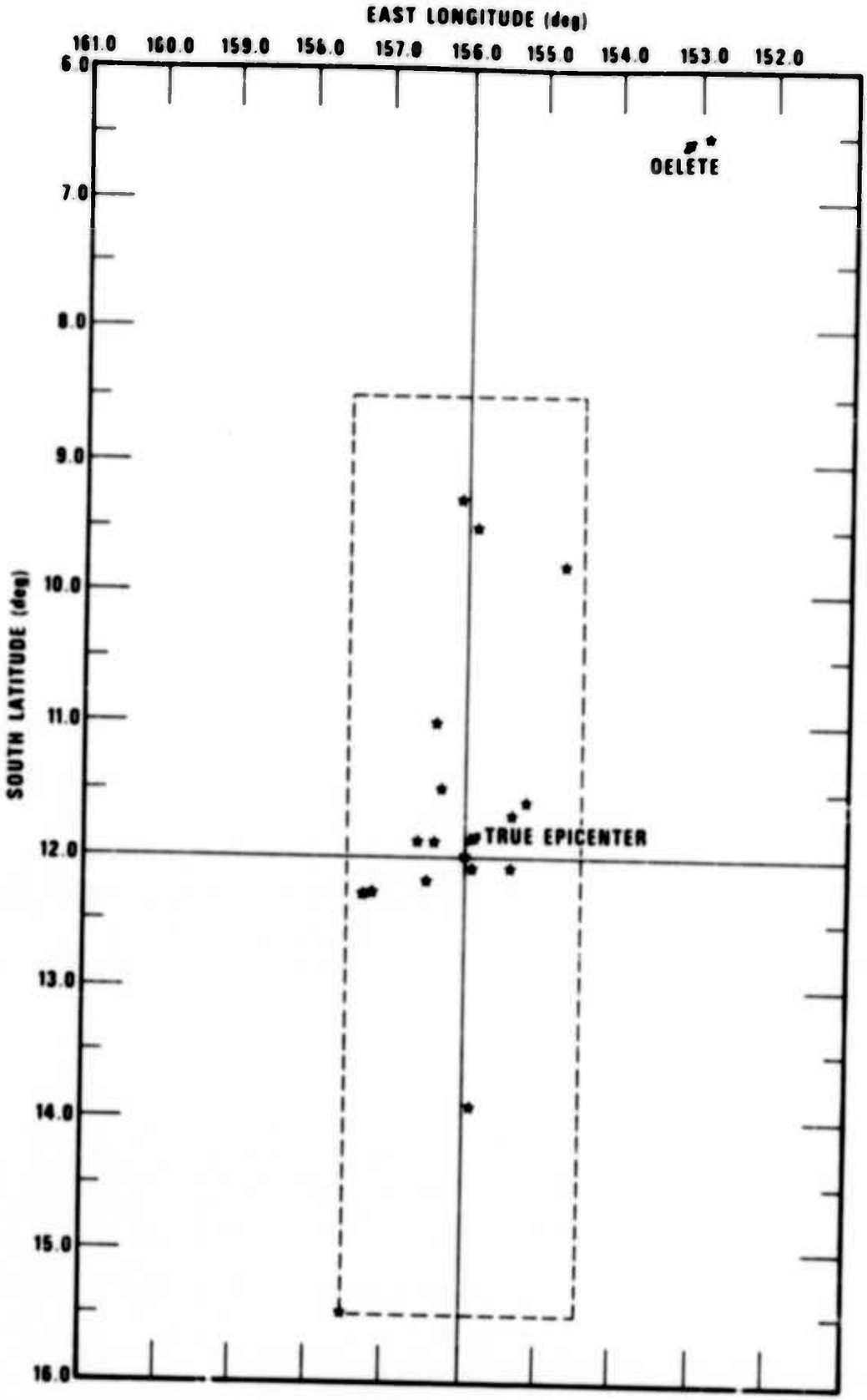

Figure A1. Location solutions, Solomon Islands - New Hebrides (12°S, 156°E).

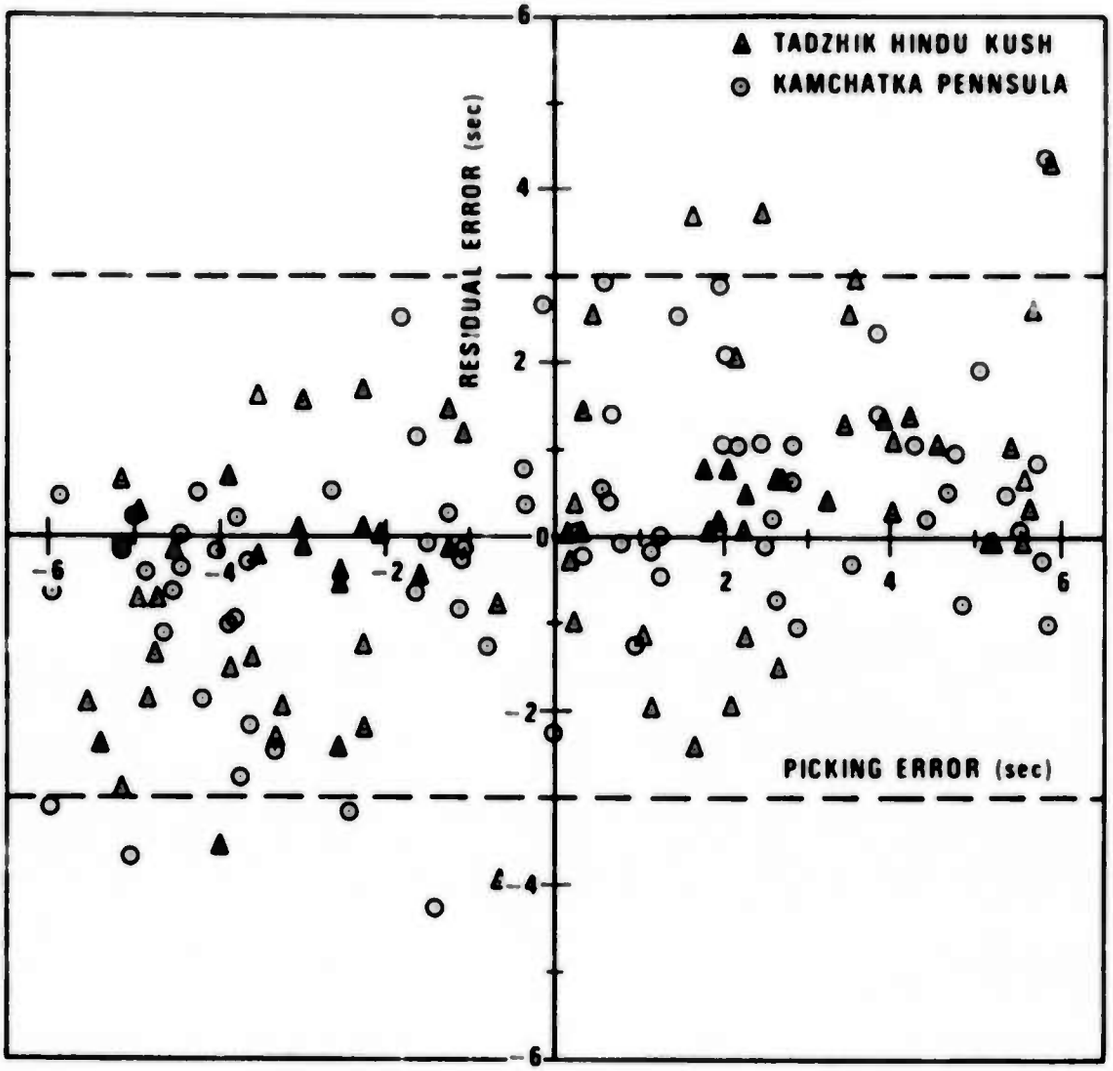

Figure A2. Comparison of residual travel-time errors and arrival-time picking errors ($-6 < \delta_i < 6$ seconds).

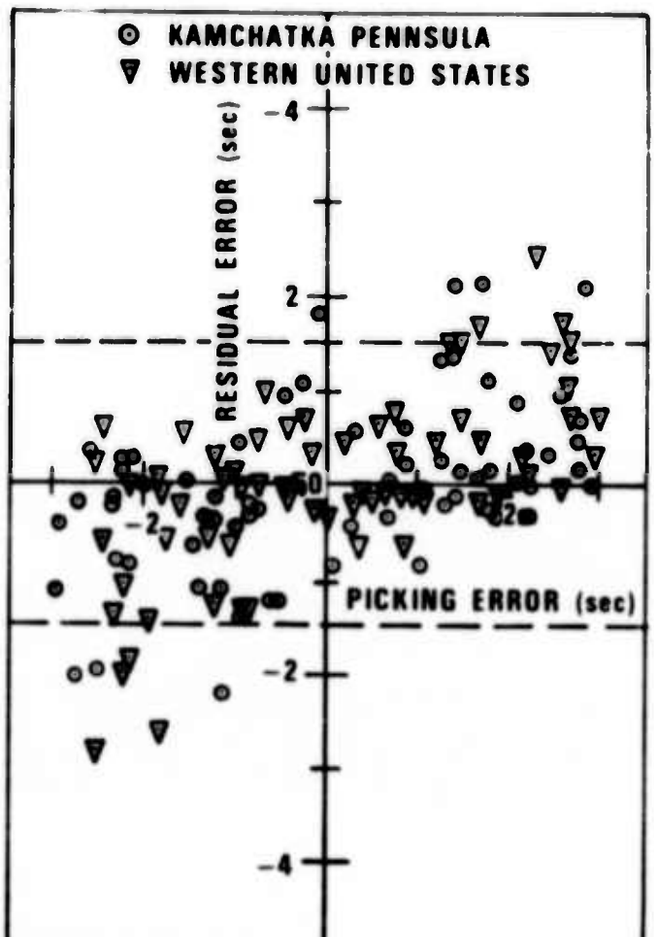

Figure A3. Comparison of residual travel-time errors and arrival-time picking errors ($-3 < \delta_i < 3$ seconds).